# Local structure and ferromagnetic character of Fe-B and Fe-P amorphous alloys

M. L. Fdez-Gubieda, A. García-Arribas, J. M. Barandiarán, and R. López Antón
*Departamento de Electricidad y Electrónica, Universidad del País Vasco, Apartado 644, 48080 Bilbao, Spain*

I. Orue and P. Gorria
*Departamento de Física, Universidad de Oviedo, Avenida Calvo Sotelo s/n, 33007 Oviedo, Spain*

S. Pizzini and A. Fontaine
*Laboratoire de Magnetisme Louis Néel, CNRS, BP 166, Avenue des Martyres, 38042 Grenoble, France*
(Received 4 August 1999; revised manuscript received 2 March 2000)

We present clear experimental evidence that the dissimilar magnetic behavior of Fe-B and Fe-P amorphous alloys is connected with differences in the local structure around Fe atoms and with the different ferromagnetic character that these systems present. Structural parameters, obtained by x-ray absorption fine structure, show that Fe-Fe nearest distances are responsible for the behavior of the Curie temperature. Both magnitudes increase with increasing the metalloid content for Fe-B and remain constant for Fe-P. The results from x-ray magnetic circular dichroism reveal that Fe-B behaves as a weak ferromagnet in all the composition range while Fe-P evolves from a weak to strong ferromagnetism character when P concentration increases. This fact determines the behavior of the magnetic moment with increasing metalloid content that displays a large decrease for Fe-P and a negligible variation for Fe-B.

Metal-metalloid Fe based amorphous alloys have been the subject of considerable research activity for the last two decades, due to the interest offered to potential applications by their outstanding magnetic properties. A great amount of experimental data has been gathered[1,2] and some elaborate theoretical investigations have been accomplished.[3,4] However, a plain examination of the contrasted behavior of two simple systems such as amorphous Fe-B and Fe-P alloys, and the divergent explanations offered by the proposed theories, suffice to show that the magnetism of $3d$ amorphous alloys is still far from being understood. In fact, a review of the magnetic properties of these two systems as a function of the composition reveals that surprisingly they behave in quite a different way. In the amorphous range of compositions, when increasing the metalloid content from 15 to 23 at. %, the Curie temperature $T_C$ remains nearly constant for Fe-P,[5,6] while increases substantially in the case of Fe-B.[6–8] At the same time, the magnetic moment per Fe atom presents a linear decrease with increasing P content in Fe-P,[5] while changing only slightly with the B concentration in Fe-B.[9] Different explanations have been proposed to justify these behaviors. Chen[10] defends that the evolution of $T_C$ relies on the dependence of the exchange integral $J_{ex}$ on the interatomic distances between magnetic atoms. Considering that, in the Bethe-Slater curve, Fe lies in the region of positive slope, this explanation qualitatively implies that an increase of $T_C$ (and therefore of $J_{ex}$) must be caused by an increase of Fe-Fe interatomic distances. A different approach is used by Hasegawa and Ray[7] who interpret the behavior of the Curie temperature in terms of a mean-field theory and suggest that possible changes in the Fe-Fe coordination number are responsible for the variation of $T_C$. On the other hand, the evolution of the magnetic moment has been usually explained in terms of the charge transfer model. Wohlfarth,[11] in the framework of itinerant ferromagnetism, favors the hypothesis that the Fe-B system behaves as a strong ferromagnet, based on the opposed variation of the saturation magnetization and the Curie temperature. However, recent calculations of the electronic structure on Fe-B and Fe-P amorphous alloys does not clarify the ferromagnetic character of Fe in these alloys. Bratkovsky and Smirnov[12] affirm that the amorphous iron borides are strong ferromagnets while Fujiwara[13] and Hafner, Tegze, and Becker[14] conclude that both systems are weak ferromagnets. It is evident that this feature, weak or strong ferromagnetism, plays a determinant role in the evolution of the Fe magnetic moment when it alloys with metalloids.

On the theoretical side, the two basic frameworks, localized and itinerant magnetism, have been specifically applied to develop theories that explain the magnetic behavior of the amorphous ferromagnetic alloys. In short, Corb, O'Handley, and Grant,[3] using the theory of localized magnetism, developed the *coordination-bond model* which attributes the magnetic to the local atomic environment, whereas, Malozemoff, Williams, and Moruzzi[4] established, in terms of the *band-gap theory*, that the magnetic properties are independent of the local environment and depend only on the valence of the metalloid. Both models make use of the fundamental assumption that the ferromagnetism is of a strong character but neither one is capable to offer a complete explanation of the composition dependence of the magnetic properties, especially on the Fe based amorphous alloys like Fe-B and the Fe-P systems.[15]

With all these considerations in mind, to progress in the analysis and understanding of the magnetic behavior of Fe based amorphous alloys, it seems imperative to reach a conclusive determination of:

(i) the exact evolution of the atomic structure with composition and its relation with the behavior of the magnetic properties, and

(ii) the ferromagnetic nature (strong or weak) of the Fe containing amorphous alloys and its concomitant implications on the magnetic behavior.

 

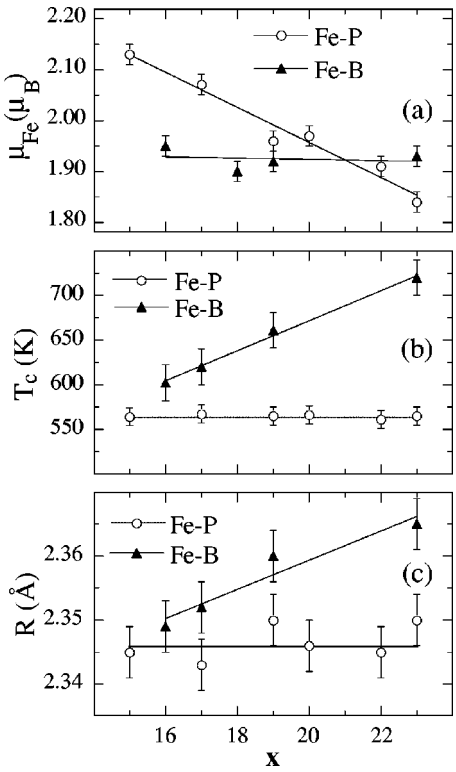


FIG. 1. Dependence on the metalloid content $x$ for $Fe_{100-x}B_x$ and $Fe_{100-x}P_x$ amorphous samples, of: (a) magnetic moment of Fe $\mu_{Fe}$, (b) Curie temperature $T_C$, and (c) nearest Fe-Fe interatomic distance $R_{Fe-Fe}$. For the Fe-P system, values for $x=17$, 19, 20, and 22 have been taken from Ref. 5.

To accomplish both goals we have studied two series of samples, $Fe_{100-x}B_x$ prepared by melt spinning and $Fe_{100-x}P_x$ by electrodeposition, in the same range of metalloid concentration $15 \leqslant x \leqslant 23$. The very same set of samples was used in all the experiments in order to avoid deceptive results caused by possible variations in sample characteristics. The investigations included: local structure determination by extended x-ray-absorption fine-structure (EXAFS) spectroscopy, x-ray magnetic circular dichroism (XMCD) at the Fe $K$ edge to determine the ferromagnetic nature of the Fe atoms, and magnetic measurements to obtain the magnetic moment per Fe atom $\mu_{Fe}$ and the Curie temperature $T_C$ for all the samples. The latter ones were obtained using a superconducting quantum interference device (SQUID) and a Faraday magnetometer. The results are displayed in Figs. 1(a) and (b). They are in complete agreement with those presented previously in the literature, which in turn, confirms that our samples are correct. We shall therefore focus in the description of the two first experiments, EXAFS and XMCD.

In amorphous materials, the lack of translational symmetry makes difficult the description of the atomic arrangement. The relevant information (and the only that can usually be obtained) is the radial distribution function around each species in the sample specified by the number and type of neighbors and their bonding distances. EXAFS is an atom selective, local probe that has proven as a useful tool for this task in this kind of systems. Using this technique, in the case of the Fe-P system, the structure of two new samples have been studied ($x=15$ and 23), expanding previous structural results (for $17 \leqslant x \leqslant 22$), which are presented in length in Ref. 5. For the Fe-B samples, the present work represents a systematic study of the structure in a set of samples that covers a wide range of compositions.

The spectra on the Fe $K$ absorption edge for both systems were recorded at room temperature at the Daresbury Synchrotron Radiation Source in the usual transmission geometry, using a Si (111) monochromator, with the storage ring operating at an energy of 2 GeV and a stored current of about 150 mA. From the experimental absorption curves, the normalized EXAFS functions $\chi(k)$ were extracted using the standard procedure.[16] The absorption above the edge was fitted using a three cubic spline up to 12 $Å^{-1}$ (the EXAFS oscillations become strongly damped above that value due to the great structural disorder). The origin of the $k$ space was taken at the inflection point of the absorption edge. The Fourier transform of $\chi(k)$, was then obtained with a $k^3$ weight and a Hanning window function. For all the samples it presents a single peak, characteristic of amorphous metallic alloys. By performing an inverse Fourier transform of this peak, a filtered EXAFS function $\chi^F(k)$ is obtained. The extraction of structural data from EXAFS experiments is performed by comparing this filtered function with a structural model using a least-squares fitting. In the framework of a dense random packing of hard spheres model, De Crescenzi *et al.*[17] proposed an expression for the radial distribution function that takes into account the characteristic asymmetric of amorphous samples and has been proved to give good results in other amorphous systems.[5,18,19] In this model, the structural parameters that describe the atomic distribution are: $N_j$, the number of neighbors of $j$ type around the absorbing species; $R_j$, the distance between the centers of the two touching spheres (that is, the nearest distance between atoms); and $\sigma_{D_j}$, the root-mean-square deviation of the distribution of distances. Note that, in this model, the average distance from the absorbing atom to its $j$ type neighbors is given by $\overline{R_j}=R_j+\sigma_{D_j}$. In conventional x-ray-diffraction experiments, this average distance is the only one that can be obtained. Using the proposed radial distribution function, the theoretical EXAFS function used in the fitting is given by[17]

$$k\chi(k)=\sum_j \frac{N_j f_j(k,\pi)}{R_j^2}\frac{e^{-2\sigma_j^2k^2}e^{-2\Gamma_j/k}}{\sqrt{1+4k^2\sigma_{D_j}^2}} \times \sin[2kR_j+\tan^{-1}(2k\sigma_{D_j})+\phi_j]. \quad (1)$$

In this expression, other terms are included, such as the amplitude and phase of backscattering, $f_j(k,\pi)$, and $\phi_j$, which have been taken from FEFF6 codes.[20] The inelastic losses terms, $\Gamma_j$ and $S_0^2$,[21] and the Debye Waller factor ($\sigma_j$) have been optimized using bcc-Fe, $Fe_2B$, $Fe_2P$ as reference compounds, as explained in Ref. 19. The uncertainty analysis was performed following Lytle, Sayers, and Stern.[22] The estimated errors are the standard ones for EXAFS: about 10% for the coordination number and $\pm 0.03$ Å for the average distances. It is to be noted that the experiment and the fitting procedure turned out to be very sensitive to the nearest interatomic distance $R_j$, which is found with much greater accuracy ($\pm 0.005$ Å). A detailed explanation of the both fitting procedure and uncertainty analysis can be found elsewhere.[23] Best-fit parameters are presented in Table I. It is

TABLE I. Structural parameters from EXAFS on Fe *K* edge for Fe-B and Fe-P amorphous samples. The values in brackets show the estimated errors in the least significant figure. All distances are given in Å.

| Sample | $N_{Fe-Fe}$ | $R_{Fe-Fe}$ | $\sigma_{D_{Fe-Fe}}$ | $\overline{R}_{Fe-Fe}$ | $N_{Fe-B}$ | $R_{Fe-B}$ | $\sigma_{D_{Fe-B}}$ | $\overline{R}_{Fe-B}$ |
|---|---|---|---|---|---|---|---|---|
| $Fe_{84}B_{16}$ | 10.4(6) | 2.349(6) | 0.23(2) | 2.58(3) | 2.0(6) | 2.20(3) | 0.02(3) | 2.22(6) |
| $Fe_{83}B_{17}$ | 10.5(7) | 2.352(7) | 0.21(2) | 2.56(3) | 2.2(6) | 2.18(3) | 0.02(4) | 2.20(7) |
| $Fe_{81}B_{19}$ | 10.6(7) | 2.360(5) | 0.20(1) | 2.56(2) | 2.5(7) | 2.18(3) | 0.05(5) | 2.23(8) |
| $Fe_{77}B_{23}$ | 10.7(7) | 2.365(6) | 0.20(2) | 2.57(3) | 3.2(7) | 2.15(4) | 0.09(4) | 2.24(8) |
| Sample | $N_{Fe-Fe}$ | $R_{Fe-Fe}$ | $\sigma_{D_{Fe-Fe}}$ | $\overline{R}_{Fe-Fe}$ | $N_{Fe-P}$ | $R_{Fe-P}$ | $\sigma_{D_{Fe-P}}$ | $\overline{R}_{Fe-P}$ |
| $Fe_{85}P_{15}$ | 10.2(5) | 2.345(3) | 0.31(1) | 2.65(3) | 2.2(6) | 2.20(2) | 0.18(6) | 2.38(6) |
| $Fe_{81}P_{19}$[a] | 10.2(6) | 2.350(4) | 0.26(1) | 2.61(4) | 2.3(6) | 2.20(2) | 0.18(6) | 2.38(6) |
| $Fe_{77}P_{23}$ | 10.4(6) | 2.350(4) | 0.22(2) | 2.57(4) | 3.1(6) | 2.19(3) | 0.25(6) | 2.44(6) |

[a]From Ref. 5.

observed that, within the error bar, there is no change in the Fe coordination number $N_{Fe-Fe}$ for none of the systems regardless of the P or B concentration, while the number of the metalloids around Fe, $N_{Fe-B(P)}$, increases with increasing the metalloid content in the sample, following their stoichiometry. The closest metal-metalloid distances $R_{Fe-B(P)}$ remains unaltered (around 2.2 Å) indicating the covalent character of the bonds, as proposed from electronic structure calculations.[12–14] The distribution of distances corresponding to P atoms in the Fe-P system present a higher degree of disorder (greater $\sigma_{D_{Fe-P}}$) than the one for the B atoms in Fe-B ($\sigma_{D_{Fe-B}}$), giving rise to a larger average distance.

The more striking difference between the two systems is the notably distinct behavior of the Fe-Fe nearest interatomic distance $R_{Fe-Fe}$. In the case of the Fe-P samples, this value does not experience any appreciable change in the whole range of composition, while for the Fe-B ones $R_{Fe-Fe}$ increase with increasing the B content. This contrasted behavior can be clearly observed in Fig. 1(c). If we also consider the structural disorder, the average interatomic distance decreases with increasing metalloid content for Fe-P and remains constant for Fe-B. The results presented in Table I (that in the case of Fe-P extend the study of Ref. 5, displaying the same trend encountered there) are very similar to those already found by diffraction techniques: $\overline{R}_{Fe-Fe}=2.61$ Å and $\overline{R}_{Fe-P}=2.38$ Å for $Fe_{82}P_{18}$,[24] $\overline{R}_{Fe-Fe}=2.56$ Å for $Fe_{80}B_{20}$,[25,26] and $Fe_{83}B_{17}$.[24,27]

The important information drawn from these structural results is that there exist a clear correlation between the evolution with composition of the Curie temperature $T_C$ and the Fe-Fe interatomic distance that can be directly observed in Figs. 1(b) and (c): when the Fe-Fe interatomic distance increases, as is the case for Fe-B, so does $T_C$, while the constancy of $R_{Fe-Fe}$ comes along with an insensitive dependence of $T_C$ on P content in Fe-P. This evidence proves that the approach of Chen[10] (that attributes the behavior of $T_C$ to the dependence of the integral exchange on the interatomic distance between magnetic atoms) is more satisfactory than the one of Hasegawa and Ray[7] (because the number of Fe-Fe neigbors does not change).

We shall now describe the XMCD experiments performed on Fe *K* edge to reveal the ferromagnetic character of the Fe-P and Fe-B systems. X-ray magnetic circular dichroism is the difference of the absorption of circularly polarized x rays when the absorbing material is magnetized antiparallel and parallel to the incident x-ray beam. This difference is caused by the different final states that the photoelectron can reach according with the applicable selection rules. X-ray absorption at the *K* edge of 3*d* transition metals involves electronic transitions from 1*s* to 4*p* final states and different theories have been proposed to interpret the results. Igarashi and Hirai[28] suggest that the XMCD signal is generated by the 3*d* orbital moment on the neighboring sites through the *p*-*d* hybridization, while Guo[29] indicates that the *K* edge XMCD spectrum probes the *p*-projected orbital magnetization density of unoccupied states. Even though the interpretation of the *K* edge XMCD is not completely clear, the features of the measured XMCD signal can be used as a fingerprint to determine the ferromagnetic character of the sample. The XMCD spectrum of pure Fe, a weak ferromagnetic system for which neither majority nor minority spin bands are full, exhibits both a positive and a negative peak, while Co and Ni, strong ferromagnets for which majority-spin band is full, present only a negative peak (see Fig. 2). It is accepted that the positive peak is related with the density of unoccupied spin-up *d* states close to the Fermi level, while the negative peak observed at higher energies is related to the density of unoccupied spin-down *d* states.[30–32] We shall take advantage of this distinct feature to distinguish without ambiguities the ferromagnetic nature of Fe in Fe-B and Fe-P amorphous systems.

The Fe *K* edge XMCD signals of Fe-B and Fe-P amorphous samples have been recorded on the energy-dispersive beamline (ID24) at the European Synchrotron Radiation Facility (ESRF). The linear polarization delivered by the plane undulator was transformed into circular polarization (PC $>$ 95%) using a diamond crystal as quarter wave plate.[33] In the geometry used, the orientation of the 0.7-T magnetic field, applied perpendicular to the sample plane, was alternatively changed with respect to the incident radiation. In this way, the spin-dependent absorption coefficient was obtained as the difference of the absorption spectra measured for parallel and antiparallel orientation of the incident photon helicity with respect to the magnetic field. The absence of mechanical movement and the parallel acquisition using a charge-coupled device camera insures the high stability necessary to detect differences in absorption as small as $10^{-3}$. The obtained XMCD signals, normalized to the edge jump of the absorption spectra, are presented in Fig. 2. The origin of the energy has been taken at the inflection point of the absorp-

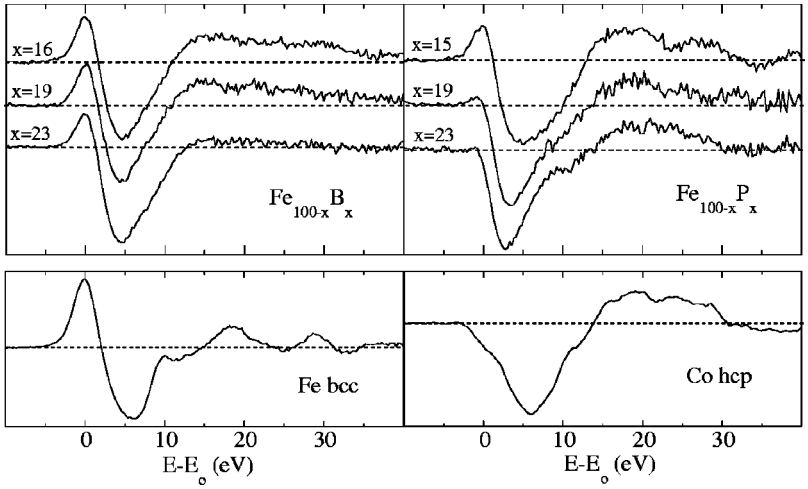


FIG. 2. Fe *K*-edge dichroism signal for $Fe_{100-x}B_x$ and $Fe_{100-x}P_x$ amorphous samples. Below, the signals from pure Fe and Co are displayed for comparison.

tion edge. It is clearly observed that the evolution of the XMCD signal differs considerably for both systems. For $Fe_{100-x}P_x$, the shape of the XMCD signal depends strongly on phosphorous concentration. For $x=15$, the XMCD signal presents both positive and negative peaks centered at 0 and 6 eV, respectively, but, when the P content is increased, the positive peak progressively disappear denoting an evident transition from weak to strong ferromagnetism. The position of the negative peak is shifted towards lower energies (from 6 eV for $x=15$ to 3 eV for $x=23$) while its width increases. In contrast, $Fe_{100-x}B_x$ display an unchanging XMCD signal for all the samples, with a positive peak centered at the absorption edge and a negative one 5 eV above, evidencing the weak character of the magnetism in all the composition range. No changes of the position of the peaks are observed for Fe-B.

The evident differences in the evolution of the XMCD and consequently in the nature of the ferromagnetism in Fe-P and Fe-B, relate directly with the distinct behavior of the magnetic moment when the metalloid content varies. A deeper insight in the origin of this contrasted behavior can be obtained considering the degree of electronic transference from the metalloid to the $3d$ band of Fe, as deduced from the $^{57}$Fe Mössbauer spectroscopy through the evolution of the isomer shift of the Fe nuclear energy levels. This parameter is proportional to the $3d$ electronic population at the Fe atoms and its increase is considerably larger in the Fe-P system [0.02 mm/s per % P (Refs. 34 and 35)] than in Fe-B [0.005 mm/s per % B (Ref. 36)] in the same range of metalloid concentration. In Fe-P, the change from a weak to strong ferromagnetism is likely due to the displacement of the Fermi level to higher energies as a consequence of the increase of the electronic charge transfer. On the contrary, for the Fe-B system, the charge transfer between Fe and B, if exists, is very small and the Fermi level moves only slightly. Fe-B samples retain the weak ferromagnetic character and as a result, the change of the Fe magnetic moment is very small. Note that, in the low metalloid composition range (around $x=16$), both systems are weak ferromagnets and also the nearest Fe-Fe distances are similar for both. However, this does not imply that the electronic structure of both systems is similar. In fact, the marked differences in the magnetic moment and the isomer shift point in the opposite direction. The Curie temperature seems to be insensitive to the charge transfer to the $3d$ band of the Fe atom as it was already noted earlier for crystalline Fe-Ni-C alloys.[37]

In conclusion, we have obtained explicit experimental evidence of the differences that Fe-B and Fe-P amorphous alloys present in their structure and ferromagnetic character. We have correlated them and their evolution when increasing the metalloid content with the different magnetic properties that these systems present. The behavior of the Curie temperature is connected with the Fe-Fe nearest distances in the atomic distribution, rather than with the number of Fe-Fe neighbors. In this way, both magnitudes increase with B content in Fe-B alloys and remain unchanged in Fe-P for all compositions. On the other hand, the ferromagnetic nature of Fe defines the evolution of the magnetic moment. Fe-B samples are weak ferromagnets in all the composition range, while a transition from weak to strong ferromagnetism is observed in Fe-P. Our results clarify the confused situation existing about this kind of systems, and reveal the actual structural and magnetic features on which models and theoretical approachs must rely.

This work was supported by the Spanish CICyT under Project Nos. MAT97-0987 and MAT99-0667.

[1] *Amorphous Metallic Alloys*, edited by F.E. Luborsky (Butterworths, London, 1983).

[2] *Glassy Metals: Magnetic, Chemical and Structural Properties*, edited by R. Hasegawa (CRC, Boca Raton, FL, 1983).

[3] B.W. Corb, R.C. O'Handley, and N.J. Grant, Phys. Rev. B **27**, 636 (1983).

[4] A.P. Malozemoff, A.R. Williams, and V.L. Moruzzi, Phys. Rev. B **29**, 1620 (1984).

[5] A. García-Arribas, M.L. Fdez-Gubieda, I. Orue, J.M. Barandiaran, J. Herreros, and F. Plazaola, Phys. Rev. B **52**, 12 805 (1995).

[6] F.E. Luborsky, J.L. Walter, and E.P. Wohlfarth, J. Phys. F **10**,

959 (1980).
[7] R. Hasegawa and R. Ray, J. Appl. Phys. **49**, 4174 (1978).
[8] C.L. Chien and K.M. Unruh, Phys. Rev. B **24**, 1556 (1981).
[9] Ze Xianyu, Y. Ishikawa, F. Fukunaga, and N. Watanabe, J. Phys. F **15**, 1799 (1985).
[10] H.S. Chen, Phys. Status Solidi A **17**, 561 (1973).
[11] E.P. Wohlfarth in *Amorphous Metallic Alloys* (Ref. 1), Chap. 15, p. 289.
[12] A.M. Bratkovsky and A.V. Smirnov, J. Phys.: Condens. Matter **5**, 3203 (1993).
[13] T. Fujiwara, J. Phys. F: **12**, 661 (1982).
[14] J. Hafner, M. Tegze, and Ch. Becker, Phys. Rev. B **49**, 285 (1994).
[15] R.C. O'Handley, J. Appl. Phys. **62**, R15 (1987).
[16] B. Lengeler and P. Eisenberger, Phys. Rev. B **21**, 4507 (1980).
[17] M. De Crescenzi, A. Balsatori, F. Comin, L. Incoccia, S. Mobilio, and N. Motta, Solid State Commun. **37**, 921 (1981).
[18] P. Lagarde, J. Rivory, and G. Vlaic, J. Non-Cryst. Solids **57**, 275 (1983).
[19] M.L. Fdez-Gubieda, I. Orue, F. Plazaola, and J.M. Barandiarán, Phys. Rev. B **53**, 620 (1996).
[20] J. Mustre de Leon, J.J. Rehr, R.C. Albers, and S.I. Zabinsky, Phys. Rev. B **44**, 4146 (1991).
[21] The value of $S_0^2$, that does not appear explicitly in Eq. (1), is already introduced in the amplitude calculation. We obtain a value for $S_0^2$ by fitting the standard compounds and recalculate the amplitudes for the problem samples introducing this value in the FEFF input.
[22] F.W. Lytle, D.E. Sayers, and E.A. Stern, Physica B **158**, 701 (1989).
[23] A. García-Arribas, M.L. Fdez-Gubieda, and J.M. Barandiarán, Phys. Rev. B **61**, 6238 (2000).
[24] Y. Waseda and H.S. Chen, Phys. Status Solidi A **49**, 387 (1978).
[25] P. Lamparter, W. Sperl, E. Nold, G. Rainer-Harbach, S. Steeb, in *Rapid Quenched Metals IV*, edited by T. Masumoto and K. Suzuki (The Japan Institute of Metals, Sendai, 1982), p. 343.
[26] P. Lamparter, W. Sperl, S. Steeb, and J. Blétry, Z. Naturforsch. **37A**, 1223 (1982).
[27] T. Fujiwara, H.S. Chen, and Y. Waseda, J. Phys. F **11**, 1327 (1981).
[28] J. Igarashi and K. Hirai, Phys. Rev. B **50**, 17 820 (1994).
[29] G.Y. Guo, J. Phys.: Condens. Matter **8**, L747 (1996).
[30] S. Pizzini, A. Fontaine, E. Dartyge, C. Giorgetti, F. Baudelet, J.P. Kappler, P. Boher, and F. Giron, Phys. Rev. B **50**, 3779 (1994).
[31] F. Manar, F. Baudelet, J.F. Bobo, E. Dartyge, A. Fontaine, Ch. Giorgetti, and M. Piecuh (unpublished).
[32] K.J. Gofron, C.W. Kimball, P.L. Lee, G. Jennings, and P.A. Montano, in *Proceedings of the 9th International Conference on X-ray Absorption Fine Structure, Grenoble, 1996* [J. Phys. IV **7**, C2-421 (1997)].
[33] S. Pizzini, M. Bonfim, F. Baudelet, H. Tolentino, A. San Miguel, K. Mackay, C. Malgrange, M. Hagelstein, and A. Fontaine, J. Synchrotron Radiat. **5**, 1298 (1998).
[34] The values of the isomer shift of Fe-P samples presented in Fig. 3 of Ref. 5, due to an unnoticed error, are absolute (spectrometer dependent), not relative to bcc Fe at room temperature as claimed in the text. A value of 0.11 mm/s must be added to the displayed values.
[35] E.J. Hiltunen, J.A. Letho, and L. Takacs, Phys. Scr. **34**, 239 (1986).
[36] C.L. Chien, D. Musser, E.M. Gyorgy, R.C. Sherwood, H.S. Chen, F.E. Luborsky, and J.L. Walter, Phys. Rev. B **20**, 283 (1979).
[37] M.C. Cadeville and E.P. Wohlfarth, Phys. Status Solidi A **26**, K157 (1974).